Geochimica et Cosmochimica Acta Vol. 51, pp. 2211–2217

0016-7037/87/$3.00 + .00

Heat capacities of synthetic hedenbergite, ferrobustamite, and $CaFeSi_2O_6$ glass

H. T. HASELTON, JR., R. A. ROBIE and B. S. HEMINGWAY
U.S. Geological Survey, 959 National Center, Reston, VA 22092, U.S.A.

(*Received January* 12, 1987; *accepted in revised form May* 26, 1987)

Abstract—Heat capacities have been measured for synthetic hedenbergite (9–647 K), ferrobustamite (5–746 K), and $CaFeSi_2O_6$ glass (6–380 K) by low-temperature adiabatic and differential scanning calorimetry. The heat capacity of each of these structural forms of $CaFeSi_2O_6$ exhibits anomalous behavior at low temperatures. The λ-peak in the hedenbergite heat-capacity curve at 34.5 K is due to antiferromagnetic ordering of the Fe^{2+} ions. Ferrobustamite has a bump in its heat-capacity curve at temperatures less than 20 K, which could be due to weak cooperative magnetic ordering or to a Schottky anomaly. Surprisingly, a broad peak with a maximum at 68 K is present in the heat-capacity curve of the glass. If this maximum, which occurs at a higher temperature than in hedenbergite is caused by magnetic ordering, it could indicate that the range of distortions of the iron sites in the glass is quite small and that coupling between iron atoms is stronger in the glass than in the edge-shared octahedral chains of hedenbergite.

The standard entropy change, $S^\circ_{298.15} - S^\circ_0$, is 174.2 ± 0.3, 180.5 ± 0.3, and 185.7 ± 0.4 J/mol·K for hedenbergite, ferrobustamite and $CaFeSi_2O_6$ glass, respectively. Ferrobustamite is partially disordered in Ca-Fe distribution at high temperatures, but the dependence of the configurational entropy on temperature cannot be evaluated due to a lack of information.

At high temperatures (298–1600 K), the heat capacity of hedenbergite may be represented by the equation

$$C_p^\circ\,(\text{J/mol}\cdot\text{K}) = 310.46 + 0.01257T - 2039.93T^{-1/2} - 1.84604\times10^6T^{-2}$$

and the heat capacity of ferrobustamite may be represented by

$$C_p^\circ\,(\text{J/mol}\cdot\text{K}) = 403.83 - 0.04444T + 1.597\times10^{-5}T^2 - 3757.3T^{-1/2}.$$

INTRODUCTION

THE PHASE RELATIONS of hedenbergite and ferrobustamite are geologically important as potential sources of information about the conditions of Ca-Fe skarn formation. Reactions can be written for the oxidation and sulfidation of these minerals, and reactions involving hedenbergite have been studied experimentally by GUSTAFSON (1974), BURTON *et al.* (1982), and GAMBLE (1982). We are not aware of a natural occurrence of iron-rich ferrobustamite, presumably, because cooling rates may be too low to prevent inversion to hedenbergite. For example, WAGER and DEER (1939) found hedenbergitic pyroxenes in fayalite ferrogabbros in the Skaergaard intrusion which they interpreted to be formed by inversion (see also discussion by LINDSLEY, 1967). Fe-poor ferrobustamite, on the other hand, has been reported to occur in skarns, principally in Japan (see ABRECHT, 1980, Table 1).

The melting relations and boundary for the transition of hedenbergite to ferrobustamite at high pressure in the system CaO-FeO-SiO_2 were determined by LINDSLEY (1967). The transition temperature at atmospheric pressure is 1233 K (BOWEN *et al.*, 1933) which agrees well with a projection of Lindsley's results at high pressures. Iron-poor ferrobustamite, which results from solid solution of ferrobustamite toward wollastonite, is stable at lower temperatures than the end-member composition (RUTSTEIN, 1971).

The crystal structure of the C2/c pyroxene hedenbergite has been refined at six temperatures from 297 to 1273 K by CAMERON *et al.* (1973). All Fe resides on the M(1) octahedral sites which form edge-shared, zig-zag chains in the c direction. RAPOPORT and BURNHAM (1973) determined the crystal structure of a synthetic, end-member ferrobustamite and a natural Fe-poor ferrobustamite. In this structure, Fe resides on four, crystallographically distinct octahedral sites M(1)–M(4). Iron is concentrated on the smaller, and more regular M(1) and M(3) sites in ordered ferrobustamite, but in their synthetic sample, significant amounts of Fe were also present on M(2) and M(4). The larger, irregular M(2) and M(4) sites coordinate loosely with additional oxygens yielding 7- and 8-fold coordination, respectively. Despite the problems posed by using a heavily twinned sample, which lowered the quality of their refinement, RAPOPORT and BURNHAM (1973) concluded that Fe tended to order onto the M(3) site in Fe-poor ferrobustamite. In a structural study of a higher quality, natural Fe-poor ferrobustamite crystal, YAMANAKA *et al.* (1977) showed that Fe segregates almost exclusively onto the M(3) site, but the Fe can be disordered significantly by a relatively short heating period at 1413 K. Therefore, the Fe distribution must be considered in phase equilibrium calculations.

Heat capacities were also measured for $CaFeSi_2O_6$ glass because the data could be useful in modelling the thermodynamic properties of compositionally complex melts.

PREVIOUS WORK

BENNINGTON *et al.* (1984) measured heat capacities (12.3–1147 K) and an enthalpy of formation by HF solution calorimetry for a natural hedenbergite sample of composition $(Ca_{.9516}Mg_{.0583}Fe^{2+}_{.7134}Fe^{3+}_{.0934}Mn_{.1366})(Si_2O_6)$ from the Laxey Mine, South Mountain, Idaho. They obtained values of

$S^\circ_{298.15} - S^\circ_0 = 172.46 \pm 0.62$ J/mol·K and ΔH°_f (1 bar, 298.15 K) = -2849.14 ± 3.58 kJ/mol; they also observed a peak in the low-temperature heat capacities at 26.5 K. O'NEILL and NAVROTSKY (1980) deduced a heat of transition from ferrobustamite to hedenbergite of 8.25 ± 1.49 kJ/mol from heats of solution in molten $2PbO \cdot B_2O_3$ at 970 K. By means of magnetic susceptibility measurements and Mössbauer spectroscopy, COEY and GHOSE (1985) determined that synthetic hedenbergite orders antiferromagnetically at 38 K.

EXPERIMENTAL PROCEDURES

Sample preparation. The $CaFeSi_2O_6$ glass was prepared from SiO_2 glass and reagent grade Fe_2O_3 and $CaCO_3$. The mix was first decarbonated at 1073 K in air and then reduced at 1223 K with a gas mixture of $CO_2/H_2 = 2.33$. A $Ag_{70}Pd_{30}$ crucible, which had been used to reduce hematite over a period of several days at the same temperature and gas mixing ratio, was used for this reduction. The reduced oxide mix was fused twice at 1573 K in a platinum crucible for about 1.5 hr per fusion in the same CO_2-H_2 gas mixture. The glass was ground coarsely between fusions, and the melt was quenched by withdrawing the crucible from the furnace and immersing it in liquid nitrogen. The color of the resulting glass was dark gray. In order to limit the absorption of iron by the crucible during the fusions, we initially treated the crucible by melting a CaO-FeO-SiO_2 mix containing about 40 wt.% FeO at 1623 K for a total of 20 hours, again, with the same gas ratio. We weighed the crucible before and after the fusions in order to have an indication, somewhat imprecise, of the absorption of iron from the starting material. During the two fusions, the crucible gained approximately 0.03 g which would correspond to about 0.6% of the total iron in the glass. If this iron metal loss were the only change in composition from ideal stoichiometry, the resulting formula would be $Ca_{1.001}Fe_{0.995}Si_{2.002}O_{6.000}$.

The hedenbergite sample was crystallized from the glass in a piston-cylinder apparatus at 9 kbar and 1273 K for 6–24 hr in graphite capsules. The yield was about 2.3 g per run. Differences in run duration did not result in noticeable changes in crystallinity. Results in THOMPSON and KUSHIRO (1972) and WOERMANN *et al.* (1977) indicate that the COH system should buffer iron in the ferrous state at the chosen *P-T* condition. The crystallized hedenbergite was in the form of green discs composed of 1–10 μm crystals. Adhering graphite was removed by repeated treatments in a low-temperature asher (International Plasma Corp.*) in which the ambient temperature was less than 373 K. The only apparent change during this process was a general lightening of color; it did not result in a yellowish tint which would suggest surface oxidation.

The hedenbergite was converted to ferrobustamite by heating at 1323 K for 20 hr in the same CO_2-H_2 gas mixture. During the conversion, the color of the material changed from green to light gray.

A small amount (<1%) of birefringent material was seen in the glass sample. It occurred in patches and the X-ray peaks indicated that it was ferrobustamite. There was no evidence of fayalite which has a heat-capacity anomaly in the same temperature range as the anomaly found in the glass. The glass heat capacities were not corrected for the presence of the ferrobustamite. No second phases were detected in either the hedenbergite or the ferrobustamite when examined with a polarizing light microscope, with powder x-ray diffraction, or in the scanning electron microscope using backscattered electron imaging. Averaged analyses for random chips of $CaFeSi_2O_6$ glass, hedenbergite, and ferrobustamite, which were obtained with an ARL-SEMQ electron microprobe (15 kV, 100 namp, 2 μm spot-size), are listed in Table 1. Synthetic fayalite was the standard for iron and natural diopside was fayalite was the standard for iron and natural diopside was used for calcium and silicon. The analyses are consistent with a $CaFeSi_2O_6$ stoichiometry within the analytical uncertainty, but the analyses are also consistent with some iron loss during fusions as discussed above. Standard deviations for CaO and FeO (Table 1) are larger for the hedenbergite and ferrobustamite analyses than those for the glass analyses. An inspection of the individual analyses of hedenbergite and ferrobustamite shows that low FeO values correspond to high CaO values. This indicates that the crystals are not as homogeneous as the glass. Unit-cell parameters were refined from x-ray data collected with Cu K_α radiation, a ⅛°/min scan rate, silicon metal (a_0 = 0.543088 nm; HUBBARD *et al.*, 1975) as an internal standard, and the refinement program written by APPLEMAN and EVANS (1973). The resulting unit-cell parameters are a = 0.9849(1) nm, b = 0.9028(1) nm, c = 0.5251(1) nm, and β = 104.91(1)° for hedenbergite and a = 0.7690(2) nm, b = 0.7112(1) nm, c = 1.3764(2) nm, α = 90.24(2)°, β = 95.20(1)°, and γ = 103.58(1)° for ferrobustamite. The molar volumes are 67.95(1) cm³ and 73.00(2) cm³ for hedenbergite and ferrobustamite, respectively. The numbers in parentheses are 1 standard deviation in the least significant figure. These parameters agree well with previous results for synthetic hedenbergite (LINDSLEY, 1967; VEBLEN and BURNHAM, 1969; CAMERON *et al.*, 1973) and synthetic ferrobustamite (RAPOPORT and BURNHAM, 1973). Bjørn Mysen (Geophysical Laboratory) collected Mössbauer spectra for the glass and hedenbergite samples at 77 and 298 K and gave the following interpretations (B. MYSEN, written communication, 1984). The Fe absorption peaks in the spectra of the glass were fit with two doublets. Although the fits to the spectra might be interpreted to indicate that two iron sites with differing degrees of distortion exist in this glass, a range of local geometries could result in similar spectra. The concentration of Fe^{3+} was less than the detection level of 2–3% of the total iron. The Mössbauer technique is more sensitive to Fe^{3+} in crystalline materials than in glasses, and the spectra of the hedenbergite indicate that 3–4% of the total iron is Fe^{3+}. The oxidation could have resulted from the synthesis at high pressures or from the ashing procedure. The hyperfine parameters for both Fe^{2+} and Fe^{3+} are consistent with network modifying Fe^{2+} and Fe^{3+} (VIRGO and MYSEN, 1985).

Table 1. Averaged electron-microprobe analyses of random chips of $CaFeSi_2O_6$ glass, hedenbergite, and ferrobustamite. Each average represents at least 15 analyses. The numbers in parentheses are one standard deviation.

Oxide	Glass	Hedenbergite	Ferrobustamite	Ideal
CaO	22.55 (0.19)	22.31 (0.52)	23.04 (0.48)	22.60
FeO	28.24 (0.26)	28.72 (0.68)	28.50 (0.59)	28.96
SiO_2	48.59 (0.47)	48.91 (0.51)	49.13 (0.43)	48.44
Total	99.38 (0.50)	99.95 (0.34)	100.67 (0.51)	100.00
Cations per 6 oxygens				
Ca	1.000	0.984	1.009	1.000
Fe	0.978	0.989	0.974	1.000
Si	2.011	2.014	2.008	2.000

Calorimetry. The low-temperature heat-capacity data were collected using an automated adiabatic calorimeter which has been described by ROBIE and HEMINGWAY (1972) and HEMINGWAY *et al.* (1984). Sample weights, corrected for buoyancy, were 17.6483 g of hedenbergite, 17.5626 g of ferrobustamite, and 23.0703 g of $CaFeSi_2O_6$ glass. Approximately 4×10^{-5} mol of helium was present in the calorimeter to promote thermal equilibration. The estimated accuracy of the C_p measurements is approximately 5% at 5 K and 0.2% at temperatures greater than 50 K. The results are listed in the chronological order of measurement in Tables 2–4 and are shown in Fig. 1 for temperatures less than 80 K. The results were smoothed using cubic splines and were extrapolated graphically

* The use of trade names is for descriptive purposes only and does not imply endorsement by the U.S. Geological Survey.

Table 2. Experimental heat capacities for synthetic hedenbergite. Series 1-3 were measured by low-temperature adiabatic calorimetry and series 4 and 5 were measured by differential scanning calorimetry.

Temp. K	Heat capacity J/(mol·K)	Temp. K	Heat capacity J/(mol·K)	Temp. K	Heat capacity J/(mol·K)
Series 1		Series 1		Series 3	
8.72	0.7420	273.28	166.3	316.41	181.0
9.59	0.9679	278.77	168.3	321.39	182.4
10.46	1.207	284.25	170.6	326.51	184.7
11.52	1.443	289.71	172.6	331.62	185.8
12.86	1.826	295.15	174.9	336.71	186.9
14.27	2.311	300.58	176.0	341.77	188.5
15.84	2.904	305.97	177.5	346.83	189.4
17.60	3.666	311.34	178.9	351.89	190.7
19.52	4.705	316.67	181.6	356.92	192.6
21.66	6.091			361.94	194.0
24.04	8.057	Series 2		366.93	195.3
26.68	10.87			371.90	196.5
29.62	15.02	24.28	8.27	376.85	197.6
32.90	21.73	25.53	9.53		
36.87	18.56	26.36	10.49	Series 4	
46.22	20.10	27.29	11.60		
51.25	23.00	28.42	13.16	339.3	187.6
57.01	27.14	29.44	14.71	349.3	190.1
63.17	32.50	30.23	16.03	359.2	192.8
69.44	37.92	30.84	17.28	369.2	195.3
75.75	43.98	31.43	18.50	379.2	198.0
81.95	49.95	31.99	19.66	389.1	200.7
88.06	55.51	32.56	20.82	399.1	202.8
94.11	60.65	33.12	21.96	409.1	204.4
100.11	65.61	33.69	23.02	419.0	206.4
106.04	70.35	34.25	23.59	429.0	209.0
111.92	74.98	34.81	23.53	439.0	210.3
117.75	79.61	35.39	22.28	448.9	211.8
123.54	84.12	35.96	20.21	458.9	214.0
129.29	88.66	36.54	18.59	468.8	215.7
135.00	93.09	37.10	18.04	478.8	217.7
140.68	97.26	37.66	17.95	488.8	219.6
146.34	101.3	38.22	18.01	497.8	220.9
151.98	105.1	39.34	18.47		
157.60	108.8	39.92	18.65	Series 5	
163.19	112.3	40.49	18.85		
168.75	115.9	41.05	19.07	468.6	215.7
174.30	119.2	41.88	18.97	478.6	217.5
179.83	122.4	42.98	19.38	488.5	217.9
185.36	125.6	44.07	19.71	498.5	218.5
190.87	128.8	45.16	19.75	508.5	220.1
196.36	131.8	46.27	20.06	518.4	220.3
201.84	134.7	47.38	20.74	528.4	221.2
207.31	137.6	48.49	21.34	538.3	222.4
212.78	140.2	49.60	21.89	548.3	222.9
218.25	143.0	50.70	22.58	558.3	224.0
223.72	145.8	52.60	23.90	568.2	224.5
229.21	148.1	55.25	25.80	578.2	225.5
234.72	150.6	57.91	27.85	588.2	226.2
240.23	153.0	60.65	30.02	598.1	227.2
245.74	155.3			608.1	228.8
251.25	157.4	Series 3		618.1	229.7
256.76	159.5			628.0	231.7
262.27	161.8	306.10	177.9	638.0	235.7
267.77	164.0	311.43	179.4	647.0	234.8

to zero kelvin by using a C_p/T *vs.* T^2 plot. Smoothed values of the heat capacity and derived thermodynamic functions are listed in Table 5–7.

High-temperature heat capacities for hedenbergite and ferrobustamite were measured with a differential scanning calorimeter following the procedures described by HEMINGWAY *et al.* (1981). The samples were contained in unsealed gold pans. We were unable to complete satisfactory scans at higher temperatures than the measured ranges because of signal instability, possibly due to oxidation of the samples. The experimental values are listed in Tables 2 and 3. At high temperatures (298–1600 K), the heat capacity of hedenbergite can be represented by

$$C_p^\circ\,(\text{J/mol}\cdot\text{K}) = 310.46 + 0.01257T - 2039.93T^{-1/2} - 1.84604\times10^6T^{-2}$$

and the heat capacity of ferrobustamite may be represented by

$$C_p^\circ\,(\text{J/mol}\cdot\text{K}) = 403.83 - 0.04444T + 1.597\times10^{-5}T^2 - 3757.3T^{-1/2}.$$

The polynomials are not strictly least-squares fits to the data. The polynomials were constrained to join the low-temperature data smoothly and to follow the heat-capacity trend of diopside at temperatures higher than the measured range. This approximation assumes that the heat capacities of oxides are additive at high temperature and that the heat capacity of diopside is a suitable guide. Note that there are no measurements at temperatures greater than 647 K for hedenbergite and 747 K for ferrobustamite. The average deviation of the polynomials to the measured data is 0.5%. The polynomials were not constrained by dummy points at temperatures greater than 1600 K.

RESULTS

The entropy change, $S^\circ_{298.15} - S^\circ_0$, is 174.2 ± 0.3, 180.5 ± 0.3, and 185.7 ± 0.4 J/mol·K for hedenbergite, ferrobustamite, and $CaFeSi_2O_6$ glass, respectively. The value of 172.46 ± 0.62 J/mol·K at 298.15 K measured by BENNINGTON *et al.* (1984) for a natural sample of hedenbergite, which differed considerably from end-member composition, and the estimated entropy of hedenbergite given by HELGESON *et al.* (1978) are close to the measured value for our synthetic sample. In hedenbergite, iron remains on the M(1) site at high temperatures (CAMERON *et al.*, 1973); therefore,

Table 3. Experimental heat capacities for synthetic ferrobustamite. Series 1 and 2 were measured by low-temperature adiabatic calorimetry and series 4-5 were measured by differential scanning calorimetry.

Temp. K	Heat capacity J/(mol·K)	Temp. K	Heat capacity J/(mol·K)	Temp. K	Heat capacity J/(mol·K)
Series 1		Series 1		Series 3	
5.36	3.090	207.46	137.7	418.8	205.4
5.85	3.380	212.96	140.3	428.7	205.8
6.43	3.414	218.44	142.8	438.7	207.5
6.97	3.718	223.91	145.5	448.7	210.3
7.75	4.067	229.39	147.7	458.6	212.0
8.61	4.338			468.6	213.2
9.59	4.589	Series 2		478.6	214.7
10.68	4.854			488.5	217.3
11.89	5.066	234.74	150.1	497.5	219.2
13.21	5.260	240.15	152.3		
14.66	5.543	245.23	153.3	Series 4	
16.25	5.762	250.29	157.4		
18.00	6.044	255.59	158.5	468.6	214.2
19.92	6.448	260.88	160.6	478.6	215.9
22.02	6.931	266.17	162.5	488.5	217.4
24.35	7.623	271.46	164.3	498.5	218.8
26.95	8.575	276.73	166.3	508.5	220.6
29.85	9.904	281.99	168.5	518.4	222.1
33.09	11.72	287.25	170.4	528.4	223.2
36.72	14.01	292.48	172.6	538.3	224.2
45.38	19.27	297.64	174.3	548.3	225.2
50.54	22.82	302.80	176.4	558.3	227.0
56.29	27.56	308.02	177.9	568.2	227.6
62.47	33.15	313.14	178.4	578.2	229.1
68.80	39.19	318.25	180.5	588.2	229.5
75.12	45.99	323.35	181.9	598.1	230.1
81.37	51.91	328.43	183.7	608.1	231.0
87.54	57.67	333.49	184.6	618.1	231.3
93.63	63.02	338.53	185.9	628.0	232.2
99.66	67.94	343.58	186.8	638.0	232.4
105.63	72.65	348.61	188.6	647.0	233.2
111.55	77.27	353.63	189.9		
117.41	81.83	358.65	190.8	Series 5	
123.23	86.34	363.64	192.3		
129.01	90.67	368.61	193.3	618.1	231.7
134.76	94.92	373.56	194.0	628.0	231.9
140.47	98.98	378.50	196.0	638.0	232.8
146.16	102.9			648.0	232.6
151.83	106.7	Series 3		657.9	233.0
157.47	110.3			667.9	232.8
163.09	113.7	339.1	187.3	677.8	233.5
168.70	116.9	349.0	190.8	687.8	234.5
174.28	120.1	359.0	192.8	697.8	235.4
179.85	123.3	369.0	194.8	707.7	236.7
185.40	126.4	378.9	197.1	717.7	238.4
190.93	129.3	388.9	198.0	727.7	240.0
196.45	132.3	398.9	200.4	737.6	242.2
201.96	135.0	408.8	202.5	746.6	243.8

Table 4. Low-temperature experimental heat capacities for $CaFeSi_2O_6$ glass.

Temp. K	Heat capacity J/(mol·K)	Temp. K	Heat capacity J/(mol·K)	Temp. K	Heat capacity J/(mol·K)
Series 1		Series 1		Series 3	
5.74	2.060	152.99	108.3	335.05	184.3
6.78	2.419	158.32	111.5	340.42	185.5
7.38	2.729	163.61	114.6	345.70	187.1
8.27	2.786	168.87	117.7	351.01	188.3
9.35	3.130	174.12	120.6	356.35	189.1
10.37	3.535	179.34	123.5	361.68	190.7
11.48	3.967	184.54	126.2	367.00	191.3
12.76	4.505	189.71	128.8	372.31	193.3
14.14	5.044	194.86	131.5	377.62	195.1
15.67	5.719	200.01	134.1	382.91	196.0
17.36	6.514	205.13	136.6		
19.24	7.450	210.23	138.9	Series 4	
21.32	8.499	215.32	141.2		
23.63	9.757			52.90	31.11
26.19	11.27	Series 2		54.02	32.38
29.03	13.44			54.95	33.47
32.23	15.35	220.36	143.6	55.91	34.38
35.82	17.88	225.39	145.7	57.01	35.89
44.25	24.11	230.36	147.8	59.18	38.57
49.25	27.62	235.35	149.8	60.28	39.19
54.78	33.30	240.39	151.7	61.38	40.28
60.75	40.20	245.42	153.7	62.46	41.49
66.96	45.78	250.44	155.8	63.54	42.74
73.28	48.49	255.45	157.8	64.63	43.60
79.50	54.28	260.46	160.0	65.71	44.46
85.51	59.57	265.49	161.8	66.79	45.37
91.44	64.54	270.55	163.5	67.86	46.48
97.36	69.26	275.59	165.3	68.94	46.72
103.19	73.62	280.62	167.4	70.03	46.04
108.94	77.87	285.63	169.0	71.11	46.42
114.62	82.11	290.63	171.0	72.19	47.28
120.25	86.17	295.62	172.5	73.25	48.28
125.82	90.21	300.60	174.0	74.33	49.22
131.34	94.14	305.56	175.5	75.40	50.39
136.82	97.91	310.51	177.0	76.46	51.51
142.25	101.5	315.44	180.2	77.53	52.55
147.64	104.9	320.36	180.4	78.61	53.48
		325.28	181.9	79.69	54.44
		330.19	183.2		

no additional entropy arises from cation disorder on the M(1) and M(2) crystallographic sites. The disordering of iron on the M(1)–M(4) sites in ferrobustamite could result in a maximum configurational contribution of $4R \ln 2 = 23.05$ J/mol·K which would be added to the measured value of 180.5 J/mol·K. It is quite possible that disorder in end-member ferrobustamite, and in Fe-poor ferrobustamite, will be variable in the temperature range of interest for phase equilibrium calculations. At present, we have information from several sources (discussed below) concerning M-site disorder in ferrobustamite, but no studies directly address the dependence of disorder on temperature.

A zero-point configurational entropy should be added to the measured values for the $CaFeSi_2O_6$ glass, but, again, the amount of this contribution is uncertain. Much additional new information would be required for an accurate calculation.

Information on disorder in synthetic ferrobustamite can be derived from a comparison of the entropy calculated from heat-capacity measurements with values calculated from phase equilibrium experiments (LINDSLEY, 1967) and with high-temperature heats of solution (O'NEILL and NAVROTSKY, 1980). LINDSLEY (1967) determined the location of the hedenbergite-ferrobustamite transition to 1543 K and 13 kbar where the transition intersects the liquidus. The boundary is well constrained by experiments, is linear within experimental uncertainty, and can be represented by the equation P (bar) = $42T$ (K) − 51800. From the slope of the boundary, we calculate an entropy of transition of 19.0 ± 0.3 J/mol·K. The entropy of transition at high pressures calculated from the heat-capacity data, assuming no disorder in ferrobustamite, is 5.7 J/mol·K, and the value is nearly constant over the temperature range of the boundary. The difference of 13.3 J/mol·K is attributed to disorder in ferrobustamite. If the disorder is distributed equally over the four M sites, the 13.3 J/mol·K corresponds to a 14% interchange

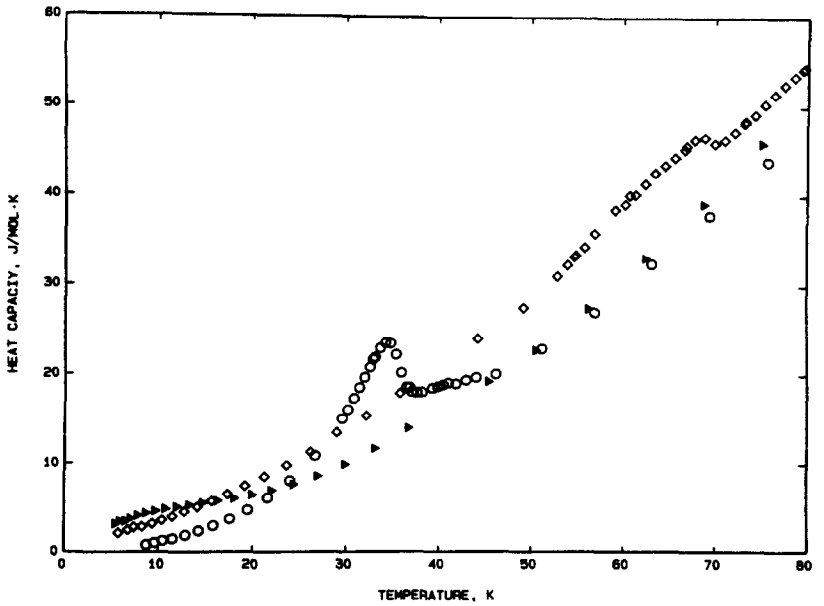

FIG. 1. Measured heat capacities at temperatures less than 80 K for $CaFeSi_2O_6$ glass, hedenbergite, and ferrobustamite. An anomaly is present in the heat capacities of each structural state of $CaFeSi_2O_6$. Circle = hedenbergite; triangle = ferrobustamite; and diamond = glass.

Table 5. Smoothed thermodynamic properties for hedenbergite. Formula weight = 248.095 g/mol.

Temp.	Heat capacity	Entropy	Enthalpy function	Gibbs energy function
T	C_P°	$S_T^\circ - S_0^\circ$	$(H_T^\circ - H_0^\circ)/T$	$-(G_T^\circ - H_0^\circ)/T$
Kelvin		J/(mol·K)		
5	0.197	0.089	0.060	0.029
10	1.097	0.446	0.312	0.134
15	2.604	1.152	0.804	0.348
20	5.050	2.204	1.532	0.672
25	9.041	3.722	2.600	1.122
30	15.74	5.904	4.178	1.726
35	22.65	9.039	6.503	2.536
40	18.71	11.58	8.064	3.516
45	20.10	13.86	9.316	4.540
50	22.16	16.05	10.47	5.585
60	29.58	20.71	13.00	7.711
70	38.53	25.93	16.00	9.933
80	48.02	31.69	19.41	12.29
90	57.13	37.88	23.10	14.78
100	65.53	44.34	26.93	17.42
110	73.52	50.96	30.80	20.16
120	81.41	57.70	34.69	23.01
130	89.21	64.52	38.58	25.94
140	96.73	71.41	42.47	28.94
150	103.8	78.33	46.33	32.00
160	110.4	85.24	50.12	35.12
170	116.6	92.12	53.85	38.27
180	122.6	98.96	57.51	41.45
190	128.3	105.7	61.08	44.65
200	133.8	112.5	64.58	47.88
210	138.9	119.1	68.00	51.11
220	143.9	125.7	71.34	54.35
230	148.5	132.2	74.59	57.59
240	152.8	138.6	77.76	60.84
250	157.0	144.9	80.85	64.07
260	161.0	151.2	83.85	67.30
270	165.0	157.3	86.78	70.52
280	168.9	163.4	89.65	73.73
290	172.6	169.4	92.44	76.93
300	175.9	175.3	95.17	80.11
310	179.1	181.1	97.83	83.27
320	182.2	186.8	100.4	86.42
330	185.2	192.5	102.9	89.55
340	187.9	198.1	105.4	92.66
350	190.6	203.5	107.8	95.75
360	193.3	208.9	110.1	98.82
370	196.0	214.3	112.4	101.9
273.15	166.2	159.2	87.69	71.54
298.15	175.3	174.2	94.67	79.52

of Fe and Ca atoms. However, the structural refinements of iron-poor ferrobustamite (RAPOPORT and BURNHAM, 1973; YAMANAKA *et al.*, 1977) indicated that Fe orders preferentially onto M(3) and preferential ordering could be expected for end-member ferrobustamite as well. In these simple calculations, we have included a thermal expansivity of 3.0×10^{-5}/K for hedenbergite (CAMERON *et al.*, 1973) and approximated the expansivity of ferrobustamite by a value of 2.4×10^{-5}/K for wollastonite (H. T. EVANS, JR, unpublished data, cited in KRUPKA *et al.*, 1979). We conclude that synthetic ferrobustamite is slightly, but significantly, disordered in experiments at high pressures in the temperature range 1223–1543 K. This conclusion is in agreement with the observation that a natural Fe-poor ferrobustamite can be partially disordered by a relatively short heating period at 1413 K (YAMANAKA *et al.*, 1977).

O'NEILL and NAVROTSKY (1980) determined an enthalpy of transition for the hedenbergite-ferrobustamite reaction by measuring heats of solution of hedenbergite and ferrobustamite in molten $2PbO \cdot B_2O_3$ at 970 K. They noted that their measured heat of transition, 8.25 ± 1.49 kJ/mol, was much less than they had expected based on the slope of the hedenbergite-ferrobustamite transition boundary. Unlike our heat-capacity measurements, the heats of solution reflect the amount of cation disorder in the sample. Their measured enthalpy of transition corresponds to an entropy of transition of 6.7 ± 1.2 J/mol · K, which indicates that their ferrobustamite sample was essentially ordered. If their ferrobustamite sample was partially disordered initially, as the phase equilibrium study by LINDSLEY (1967) would suggest, their measurements indicate that synthetic ferrobustamite may order in a few hours at 970 K, the time and temperature in the calorimeter experiments. If ferrobustamite does order during the calorimeter equilibration period, the rate of Ca-Fe interchange is fast.

The high-temperature relations of hedenbergite and ferrobustamite have been compared with those of the isostructural chemical analogues, johannsenite and bustamite. The similar slopes and volumes of transition (ANGEL, 1984) indicate that bustamite also may be partially disordered at high temperatures.

The best-characterized reaction for the calculation of the free energy and enthalpy of formation for hedenbergite involves the oxidation of hedenbergite to

Table 6. Smoothed thermodynamic properties for ferrobustamite. Formula weight = 248.095 g/mol.

Temp.	Heat capacity	Entropy	Enthalpy function	Gibbs energy function
T	C_P°	$S_T^\circ - S_0^\circ$	$(H_T^\circ - H_0^\circ)/T$	$-(G_T^\circ - H_0^\circ)/T$
Kelvin		J/(mol·K)		
5	2.925	2.464	1.419	1.045
10	4.669	5.113	2.672	2.441
15	5.591	7.190	3.500	3.690
20	6.529	8.917	4.131	4.786
25	7.906	10.51	4.739	5.772
30	10.00	12.12	5.428	6.695
35	12.87	13.87	6.281	7.594
40	15.91	15.79	7.295	8.497
45	19.03	17.84	8.424	9.418
50	22.49	20.02	9.654	10.37
60	30.84	24.83	12.46	12.37
70	40.55	30.31	15.77	14.53
80	50.56	36.38	19.50	16.88
90	59.81	42.88	23.47	19.40
100	68.23	49.62	27.53	22.09
110	76.14	56.50	31.60	24.90
120	83.87	63.45	35.63	27.82
130	91.41	70.47	39.63	30.83
140	98.63	77.51	43.59	33.92
150	105.4	84.55	47.49	37.06
160	111.8	91.56	51.31	40.24
170	117.7	98.51	55.05	43.47
180	123.4	105.4	58.68	46.72
190	128.8	112.2	62.23	49.99
200	134.0	119.0	65.70	53.27
210	138.9	125.6	69.07	56.55
220	143.6	132.2	72.35	59.84
230	148.0	138.7	75.55	63.13
240	152.2	145.1	78.65	66.41
250	156.3	151.4	81.68	69.68
260	160.2	157.6	84.62	72.94
270	164.0	163.7	87.49	76.19
280	167.8	169.7	90.29	79.42
290	171.5	175.7	93.03	82.64
300	175.0	181.5	95.70	85.84
310	178.1	187.3	98.31	89.02
320	181.0	193.0	100.9	92.18
330	183.7	198.6	103.3	95.32
340	186.3	204.2	105.7	98.44
350	188.8	209.6	108.1	101.5
360	191.2	215.0	110.3	104.6
370	193.6	220.2	112.6	107.7
273.15	165.2	165.6	88.38	77.21
298.15	174.4	180.5	95.21	85.25

Table 7. Smoothed thermodynamic properties for $CaFeSi_2O_6$ glass. Formula weight = 248.095 g/mol.

Temp.	Heat capacity	Entropy	Enthalpy function	Gibbs energy function
T	C_p°	$S_T^\circ - S_0^\circ$	$(H_T^\circ - H_0^\circ)/T$	$-(G_T^\circ - H_0^\circ)/T$
Kelvin	J/(mol·K)			
5	1.375	0.557	0.363	0.194
10	3.419	2.295	1.486	0.809
15	5.418	4.044	2.451	1.593
20	7.848	5.926	3.488	2.438
25	10.53	7.956	4.620	3.336
30	14.04	10.18	5.895	4.288
35	17.27	12.58	7.280	5.300
40	21.01	15.13	8.761	6.368
45	24.59	17.81	10.33	7.490
50	28.29	20.59	11.93	8.660
60	39.17	26.68	15.54	11.14
70	46.50	33.39	19.55	13.84
80	54.75	40.07	23.37	16.70
90	63.36	47.02	27.34	19.68
100	71.25	54.11	31.35	22.77
110	78.67	61.25	35.31	25.94
120	86.01	68.41	39.23	29.18
130	93.20	75.58	43.11	32.47
140	100.0	82.74	46.93	35.81
150	106.4	89.86	50.69	39.18
160	112.5	96.92	54.36	42.56
170	118.3	103.9	57.95	45.97
180	123.8	110.8	61.46	49.38
190	129.0	117.7	64.88	52.80
200	134.1	124.4	68.21	56.21
210	138.8	131.1	71.46	59.62
220	143.4	137.6	74.63	63.01
230	147.6	144.1	77.71	66.40
240	151.6	150.5	80.71	69.77
250	155.6	156.7	83.62	73.12
260	159.7	162.9	86.47	76.46
270	163.4	169.0	89.25	79.78
280	167.0	176.0	91.96	83.07
290	170.6	181.0	94.61	86.34
300	173.8	186.8	97.20	89.59
310	177.3	192.5	99.73	92.82
320	180.7	198.2	102.2	96.03
330	183.1	203.8	104.6	99.21
340	185.5	209.3	107.0	102.4
350	188.0	214.7	109.2	105.5
360	190.0	220.1	111.5	108.6
370	192.5	225.3	113.6	111.7
380	195.5	230.5	115.7	114.8
273.15	164.5	170.9	90.11	80.82
298.15	173.2	185.7	96.73	89.00

andradite, magnetite, and quartz. This calculation was done by ROBIE *et al.* (1987) utilizing the present heat-capacity data for hedenbergite and their new heat-capacity data for andradite. Their calculated values, based on the phase equilibrium study by BURTON *et al.* (1982), are $\Delta G^\circ_{f,298} = -2674.3 \pm 5.8$ and $\Delta H^\circ_{f,298} = -2837.6 \pm 5.8$ J/mol.

The $CaFeSi_2O_6$ composition presents an uncommon opportunity to observe the effect of structural state on magnetic behavior. An anomaly is present in each of the three low-temperature heat capacity curves (Fig. 1). The peak in the hedenbergite heat capacity curve, which occurs at 34.5 K, is the result of antiferromagnetic ordering (COEY and GHOSE, 1985). The corresponding anomaly observed in a natural hedenbergite sample by BENNINGTON *et al.* (1984) lies at a lower temperature, 26.5 K, due to the lower concentration of iron. An ill-defined bump is present in the ferrobustamite heat capacity at temperatures below 20 K. The cause of the bump could be weak cooperative magnetic ordering or a Schottky anomaly (GOPAL, 1966). A cooperative magnetic transition is expected to be hindered by the disordering of iron on four crystallographically distinct sites. Surprisingly, a broad peak with a maximum at about 68 K occurs in the heat-capacity curve of the glass. The peak probably corresponds to a magnetic transition. The presence of a magnetic transition in the glass at a higher temperature than in hedenbergite might indicate that the iron sites in the glass have a narrow range of distortion and that the coupling among iron atoms is stronger than in the edge-shared octahedral chains of hedenbergite. If the iron site in $CaFeSi_2O_6$ glass is well defined, a wide range of site distortion is not the explanation for the broadening of Fe absorption peaks in the Mössbauer spectra relative to Fe absorption peaks for hedenbergite. The broadening of the Fe absorption peaks for glasses relative to peaks for crystalline material has been observed for many silicate compositions (VIRGO and MYSEN, 1985).

Acknowledgements—We especially thank Bjørn Mysen for running and interpreting the Mössbauer scans of the hedenbergite and $CaFeSi_2O_6$ glass. We also thank I-Ming Chou, Donald H. Lindsley, Charles A. Lawson, Pascal Richet, and Alexandra Navrotsky for critical reviews of the manuscript.

Editorial handling: B. J. Wood

REFERENCES

ABRECHT J. (1980) Stability relations in the system $CaSiO_3$-$CaMnSi_2O_6$-$CaFeSi_2O_6$. *Contrib. Mineral. Petrol.* **74**, 253–261.

ANGEL R. J. (1984) The experimental determination of the johannsenite-bustamite equilibrium inversion boundary. *Contrib. Mineral. Petrol.* **85**, 272–278.

APPLEMAN D. E. and EVANS H. T. JR. (1973) Job 9214: indexing and least-squares refinement of powder diffraction data. U.S. Department of Commerce National Technical Information Service, PB2-16188.

BENNINGTON K. O., BEYER R. P. and BROWN R. R. (1984) Thermodynamic properties of hedenbergite, a complex silicate of Ca, Fe, Mn, and Mg. *U.S. Bur. Mines Rept. Inv. 8873*, 19p.

BOWEN N. L., SCHAIRER J. F. and POSNJAK E. (1933) The system CaO-FeO-SiO_2. *Amer. J. Sci.* **26**, 193–284.

BURTON J. C., TAYLOR L. A. and CHOU I. M. (1982) The f_{O_2}-T and f_{S_2}-T stability relations of hedenbergite and of hedenbergite-johannsenite solid solutions. *Econ. Geol.* **77**, 764–783.

CAMERON M., SUENO S., PREWITT C. T. and PAPIKE J. J. (1973) High-temperature crystal chemistry of acmite, diopside, hedenbergite, jadeite, spodumene, and ureyite. *Amer. Mineral.* **58**, 594–618.

COEY J. M. D. and GHOSE S. (1985) Magnetic order in hedenbergite, $CaFeSi_2O_6$. *Solid State Commun.* **53**, 143–145.

GAMBLE R. P. (1982) An experimental study of sulfidation reactions involving andradite and hedenbergite. *Econ. Geol.* **77**, 784–797.

GOPAL E. S. R. (1966) *Specific Heats at Low Temperatures.* Plenum Press, 240p.

GUSTAFSON W. I. (1974) The stability of andradite, hedenbergite, and related minerals in the system Ca-Fe-Si-O-H. *J. Petrol.* **15**, 455–496.

HELGESON H. C., DELANY J. M., NESBITT H. W. and BIRD D. K. (1978) Summary and critique of the thermodynamic properties of rock-forming minerals. *Amer. J. Sci.* **278A**, 1–229.

HEMINGWAY B. S., KRUPKA K. M. and ROBIE R. A. (1981) Heat capacities of the alkali feldspars between 350 and 1000 K from differential scanning calorimetry, the thermodynamic functions of the alkali feldspars from 298.15 to 1400

K, and the reaction quartz + jadeite = analbite. *Amer. Mineral.* **66**, 1202–1215.

HEMINGWAY B. S., ROBIE R. A., KITTRICK J. A., GREW E. S., NELEN J. A. and LONDON D. (1984) The heat capacities of osumilite from 298.15 to 1000 K, the thermodynamic properties of two natural chlorites to 500 K, and the thermodynamic properties of petalite to 1800 K. *Amer. Mineral.* **69**, 701–710.

HUBBARD C. R., SWANSON H. E. and MAUER F. A. (1975) A silicon powder diffraction standard reference material. *J. Appl. Crystall.* **8**, 45–48.

KRUPKA K. M., ROBIE R. A. and HEMINGWAY B. S. (1979) High-temperature heat capacities of corundum, periclase, anorthite, $CaAl_2Si_2O_6$ glass, muscovite, pyrophyllite, $KAlSi_3O_8$ glass, grossular, and $NaAlSi_3O_8$ glass. *Amer. Mineral.* **64**, 86–101.

LINDSLEY D. H. (1967) The join hedenbergite-ferrosilite at high pressures and temperatures. *Carnegie Inst. Wash. Yearb.* **65**, 230–234.

O'NEILL H. ST. C. and NAVROTSKY A. (1980) The thermodynamics of the clinopyroxene to pyroxenoid phase transition in the systems CaO-"FeO"-SiO_2 and CaO-MnO-SiO_2. *Eos* **61**, 1147.

RAPOPORT P. A. and BURNHAM C. W. (1973) Ferrobustamite: The crystal structures of two Ca, Fe bustamite-type pyroxenoids. *Z. Kristallogr.* **138**, 419–437.

ROBIE R. A., ZHAO B., HEMINGWAY B. S. and BARTON M. D. (1987) Heat capacity and thermodynamic properties of andradite garnet, $Ca_3Fe_2Si_3O_{12}$, between 10 and 1000 K. *Geochim. Cosmochim. Acta* **51**, 2219–2224.

ROBIE R. A. and HEMINGWAY B. S. (1972) Calorimeters for heat of solution and low-temperature heat capacity measurements. *U.S. Geol. Survey Prof. Paper 755.*

RUTSTEIN M. S. (1971) Re-examination of the wollastonite-hedenbergite ($CaSiO_3$-$CaFeSi_2O_6$) equilibria. *Amer. Mineral.* **56**, 2040–2052.

THOMPSON R. N. and KUSHIRO I. (1972) The oxygen fugacity within graphite capsules in piston-cylinder apparatus. *Carnegie Inst. Wash. Yearb.* **71**, 615–616.

VEBLEN D. R. and BURNHAM C. W. (1969) The crystal structures of hedenbergite and ferrosalite. *Can. Mineral.* **10**, 147.

VIRGO D. and MYSEN B. O. (1985) The structural state of iron in oxidized vs. reduced glasses at 1 atm: A ^{57}Fe Mössbauer study. *Phys. Chem. Minerals* **12**, 65–76.

WAGER L. R. and DEER W. A. (1939) Geological investigations in East Greenland, III. Petrology of the Skaergaard intrusion, Kangerdlugssuaq, East Greenland. *Medd. Grønland* **105**, 1–355.

WOERMANN E., KNECHT B., ROSENHAUER M. and ULMER G. C. (1977) The stability of graphite in the system C-O. Ext. Abstr., 2nd Intl. Kimberlite Conf., Santa Fe, New Mexico.

YAMANAKA T., SADANAGA R. and TAKEUCHI Y. (1977) Structural variation in the ferrobustamite solid solution. *Amer. Mineral.* **62**, 1216–1224.